where $N_{E''}$ is now a counting rate per constant energy (or range) difference.

One can also calculate the total number of electrons of energy E' which escape as a check of the above result. If this is again done for a volume with a square centimeter base at the surface, the total number of electrons of energy E' which escape from a volume element $d\tau$ at x is

$$\int_0^{2\pi}\int_0^{\cos^{-1}x/R'}\frac{N_{R'}}{4\pi}\sin\phi d\phi d\theta dx=\frac{N_{R'}}{2}\left[1-\frac{x}{R'}\right]dx.$$

Integration over x from 0 to R' gives $N_{R'}/4R'$.

If we integrate $N_{E''}$ over R'' from 0 to R' we get

$$\int_0^{R'}\frac{N_{R'}}{4}dR''=\frac{N_{R'}}{4}R',$$

as we should, since the total count due to degraded pulses should equal the total number of electrons escaping.

The above result states that electrons of energy E' which escape from the crystal are degraded with equal probability into all energies below E', since the above results are independent of E' or E''. The fraction of electrons of energy E' which escape from the crystal is equal to $\frac{1}{4}$ the fraction of the volume of the crystal which lies in a surface layer of depth R'. These two facts can be used in a graphical method to correct distorted beta-spectra for the effect due to the escape of electrons.

A similar analysis can be made for the escape of photons from a crystal, substituting an exponential absorption for the range. The solution in this case involves the Γ-function, which is somewhat awkward, but one can consult tables of this function to obtain numerical answers.

APPENDIX II

Outline of the Calculation of the Transition Energy in K Orbital Electron Capture from a Knowledge of the Branching Ratio[15]

Marshak's lifetime formulas for first-forbidden β^--decay and orbital electron capture are, respectively,

$$\frac{1}{\tau_T}=\frac{1}{\tau_0}\frac{|M|^2}{[1.3]^2}R^2B_1(z,W_0)$$

and

$$\frac{1}{\tau_c}=\frac{1}{\tau_0}\frac{|M|^2}{|1.3|^2}R^2B_c'(z,W_0),$$

where τ_0 is a decay constant, R is the nuclear radius, M is a nuclear matrix element, and the B's are quantities which depend on the order of the transition, on the nuclear charge, and on the energy difference between the parent and product nuclei.

Dividing one equation by the other one gets

$$\frac{\tau_c}{\tau_T}=\frac{B_1(z,W_0)}{B_c^{(1)}(z,W_0)}=\frac{\%\ \beta\text{ emission}}{\%\ K\text{ capture}}.$$

Except for a numerical factor, B_1 is the same function as Davidson's[7] f_1 (in the low Z limit) and can be calculated with the help of Feenberg and Trigg's[14] curves of f_0.

$B_c^{(1)}$ is given by Marshak, and for K orbital electron capture alone it has the form

$$B_c^{(1)}=\tfrac{1}{2}\pi(W_0+W_K)^4n_Kg_K^2,$$

where n_K is the number of electrons in the K shell and g_K is the "large" radial Dirac wave function, for which an expression is given by Marshak. Using these relationships one can solve for W_0.

[15] This method for calculating the transition energies was very kindly shown to us by M. Fuchs of this laboratory.

PHYSICAL REVIEW VOLUME 88, NUMBER 5 DECEMBER 1, 1952

The Strong-Focusing Synchroton—A New High Energy Accelerator*

ERNEST D. COURANT, M. STANLEY LIVINGSTON,† AND HARTLAND S. SNYDER
Brookhaven National Laboratory, Upton, New York

(Received August 21, 1952)

Strong focusing forces result from the alternation of large positive and negative n-values in successive sectors of the magnetic guide field in a synchrotron. This sequence of alternately converging and diverging magnetic lenses of equal strength is itself converging, and leads to significant reductions in oscillation amplitude, both for radial and axial displacements. The mechanism of phase-stable synchronous acceleration still applies, with a large reduction in the amplitude of the associated radial synchronous oscillations. To illustrate, a design is proposed for a 30-Bev proton accelerator with an orbit radius of 300 ft, and with a small magnet having an aperture of 1×2 inches. Tolerances on nearly all design parameters are less critical than for the equivalent uniform-n machine. A generalization of this focusing principle leads to small, efficient focusing magnets for ion and electron beams. Relations for the focal length of a double-focusing magnet are presented, from which the design parameters for such linear systems can be determined.

BETATRON OSCILLATIONS

RESTORING forces due to radially-decreasing magnetic fields lead to stable "betatron" and "synchrotron" oscillations in synchrotrons. The amplitudes of these oscillations are due to deviations from the equilibrium orbit caused by angular and energy spread in the injected beam, scattering by the residual gas, magnetic inhomogeneities, and frequency errors. The strength of the restoring forces is limited by the

* Work done under the auspices of the AEC.

† Massachusetts Institute of Technology, Cambridge, Massachusetts.

stability condition:[1] $0<n<1$, where $n=-(r/B)(dB/dr)$. Frequencies of vertical and radial oscillations are given in terms of the frequency of revolution f_0 by

$$f_z=n^{\frac{1}{2}}f_0; \quad f_r=(1-n)^{\frac{1}{2}}f_0. \tag{1}$$

The corresponding amplitudes are inversely proportional to these oscillation frequencies, for a given angular deviation. Therefore, the aperture required to accommodate either mode can only be reduced at the expense of the other mode, and the minimum aperture for both occurs with $n=0.5$.

The focusing forces can be greatly strengthened by letting n vary in azimuth. Suppose the circular orbit to consist of N sectors of equal length with n_1 and n_2 in alternate sectors. The equations of vertical and radial oscillations are then

$$d^2z/d\theta^2+n_1z=0; \quad d^2r/d\theta^2+(1-n_1)r=0; \quad \text{(odd sectors).} \tag{2a}$$

$$d^2z/d\theta^2+n_2z=0; \quad d^2r/d\theta^2+(1-n_2)r=0; \quad \text{(even sectors).} \tag{2b}$$

Solutions can be obtained by the use of recursion formulas, and are of the form

$$Z_\kappa=Ae^{i2\pi\mu_z\kappa} \quad \text{and} \quad R_\kappa=Be^{i2\pi\mu_r\kappa}, \tag{3}$$

where the coefficient μ_z is given by

$$\cos 2\pi\mu_z=\cos\frac{2\pi n_1^{\frac{1}{2}}}{N}\cos\frac{2\pi n_2^{\frac{1}{2}}}{N}-\frac{n_1+n_2}{2(n_1n_2)^{\frac{1}{2}}}\sin\frac{2\pi n_1^{\frac{1}{2}}}{N}\sin\frac{2\pi n_2^{\frac{1}{2}}}{N}. \tag{4}$$

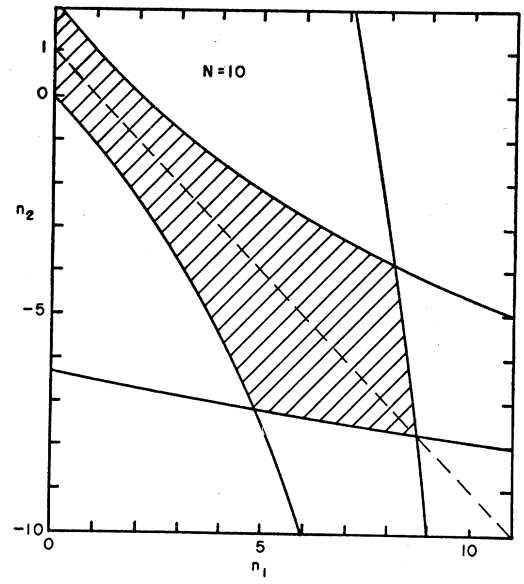

FIG. 1. Region of stability for both radial and vertical oscillations for $N=10$ sectors with n values alternating between n_1 and n_2.

[1] D. W. Kerst and R. Serber, Phys. Rev. 60, 53 (1941).

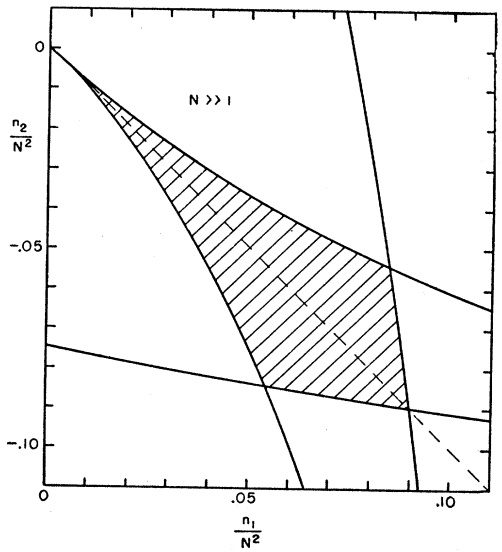

FIG. 2. Region of stability for radial and vertical oscillations for a large number of sectors N, in terms of the parameters n_1/N^2 and n_2/N^2.

The coefficient μ_r is given by the same expression, with n_1 and n_2 replaced by $(1-n_1)$ and $(1-n_2)$, respectively. If the motion is to be stable for both radial and vertical oscillations, the limits are established by the conditions

$$-1<\cos 2\pi\mu_z<1, \quad -1<\cos 2\pi\mu_r<1. \tag{5}$$

These limits have been plotted in Fig. 1 for the specific value $N=10$, and the region of stability is indicated. It is observed that the region of stability is widest for $n_2\simeq -n_1$. Figure 2 shows the stable region for very large N, and the coordinates are given in terms of n_1/N^2 and n_2/N^2. The range of stable values of n is widest when N is large and when $n_2=-n_1$, and the center of the region of stability ($\cos 2\pi\mu=0$) occurs for

$$|n|=N^2/16. \tag{6}$$

The effective frequency of the "betatron" oscillations is given by:

$$f_z=f_r=(\mu N/2)f_0 \quad \text{(for large } N\text{)}, \tag{7}$$

which can be compared with the frequencies given in Eq. (1) for constant n. Therefore, the amplitudes of oscillation and the aperture requirements can be made much smaller by the use of a large number of sectors N and correspondingly large positive and negative values of n in successive sectors. As a numerical example, consider a synchrotron of 240 alternating sectors, with $n_1=3600$ and $n_2=-3600$. The radial aperture requirement is about 1/24 that for the corresponding synchrotron with a constant n of 0.6, and 1/20 for the vertical aperture. Ion trajectories are not sinusoidal as in the standard synchrotron, but are composed of sections of alternately harmonic and hyperbolic functions. Figure 3 is a schematic illustration of two typical oscillating orbits computed for the case discussed in the

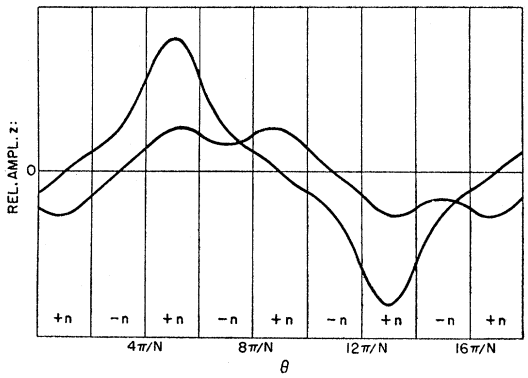

FIG. 3. Typical oscillating orbits in successive sectors at the center of the stability region ($|n|=N^2/16$), showing periodicity in 8 sectors.

foregoing showing a periodicity in 8 sectors, so there are 30 complete "betatron" oscillations around the orbit. The maximum amplitude of this nonharmonic function is found to be about twice that for a sine wave of the same frequency and starting with an equal angle at the axis. This factor has been included in estimating the aperture requirements above.

Deviations from a constant value of field gradient in the aperture have been considered. These would lead to nonlinear terms in Eq. (2). It is found that, provided the magnet sectors are symmetrical about their centerlines, such nonlinear terms do not give rise to any secular variations in the amplitudes of the oscillations. This same analysis shows that the fringing fields at the ends of the sectors, associated with the sharp change from large positive to large negative gradients, do not result in amplitudes which increase with time.

A practical requirement in the construction of such a field is that the sectors be separated by short gaps, to accommodate magnet windings, vacuum pump outlets, and other equipment. The effect of adding such short field-free sections is to change the relation given in Eq. (4) between μ and the parameters N and n, equivalent to adding terms on the right-hand side of the relation. The behavior of the betatron oscillations will be similar, and the results will not be significantly different if the length of the straight sections is less than 25 percent of that of the sectors.

SYNCHRONOUS STABILITY

The problems of "synchrotron" oscillations are the same as for the conventional proton synchrotron as discussed, for example, by Blachman and Courant,[2] except that the relation between particle energy and the circumference of the equilibrium orbit is changed. If the momentum of the particle differs from its value at the central circular orbit, the new equilibrium orbit is no longer a circle, but is a periodic alternation of harmonic and hyperbolic functions superimposed on a circle of a different equilibrium radius. The orbits for higher energy and lower energy particles than those at the central orbit are illustrated in Fig. 4, in which the curvature of the central orbit is neglected, so that it appears as a straight line. The dotted lines through the displaced orbits represent their mean radial positions. If the gradients in the two sectors are equal and opposite, the average field along these dotted lines is the same as that of the central orbit. However, the average field along the actual displaced orbit for the upper curve (energy excess) is higher than that of the dotted line in both sectors, and smaller in both sectors for the lower orbit. This illustrates the spread in mean orbit radius associated with a spread in momentum. If the momentum deviation is Δp, the fractional change in the circumference ΔL is given by

$$\Delta L/L=\alpha\Delta p/p,$$

where

$$\alpha=\frac{2-n_1-n_2}{2(1-n_1)(1-n_2)}\frac{N}{2\pi}\frac{(n_1-n_2)^2}{[(1-n_1)(1-n_2)]^{\frac{1}{2}}}\times\frac{\sin\phi_1\sin\phi_2}{(1-n_1)^{\frac{1}{2}}\sin\phi_1\cos\phi_2+(1-n_2)^{\frac{1}{2}}\sin\phi_2\cos\phi_1},\quad(8)$$

$$\phi_1=(1-n_1)^{\frac{1}{2}}\pi/N,\quad\text{and}\quad\phi_2=(1-n_2)^{\frac{1}{2}}\pi/N.$$

For our particular case, with $n_1=-n_2=N^2/16\gg1$, this reduces to

$$\alpha=4.85/|n|,\quad(9)$$

while for a conventional synchrotron $\alpha=(1-n)^{-1}$.

Synchrotron stability is governed by the change of the period of revolution with momentum. In the standard synchrotron a particle with excess momentum traverses a path of larger radius and requires a longer time, since the relative increase in radius is greater than the relative increase in velocity. This is evident from the relation

$$\frac{\Delta t}{t}=\frac{\Delta L}{L}-\frac{\Delta v}{v}=\left(\alpha-\frac{E_0^2}{E^2}\right)\frac{\Delta p}{p}=\gamma\frac{\Delta p}{p},\quad(10)$$

where E_0 and E are the rest energy and total energy of the particle, respectively. In our case α is very small if

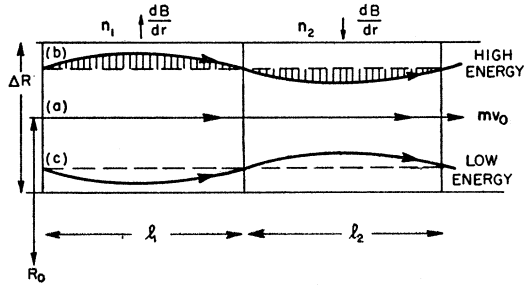

FIG. 4. Stable synchronous orbits in the radial aperture of the strong-focusing synchrotron. Higher energy particles traverse an average magnetic field larger than that at the central orbit, and vice versa, which leads to the strong radial compaction of orbits.

[2] N. M. Blachman and E. D. Courant, Rev. Sci. Instr. **20**, 596 (1949).

$|n|$ is large, so γ is negative for low particle energies, and changes sign at an energy $E_1=E_0/\alpha^{\frac{1}{2}}$, while for the ordinary synchrotron γ is always positive.[3] This means that acceleration occurs on the rising side of the voltage wave for low energies. For example, if the peak voltage is twice the mean energy increment per turn, the equilibrium phase angle is 30° as against 150° for the conventional synchrotron. This leads to electrical defocusing, as in the linear accelerator, but is more than compensated by the strong magnetic focusing described earlier.

As the energy passes through the value E_1, the equilibrium phase angle shifts from the rising to the falling slope of the voltage curve. At this point the frequency is independent of radius and of energy, as in the modification of the fixed-frequency cyclotron proposed by Thomas.[4] This transition occurs at a rather large energy. For example, in the design study for a 30-Bev accelerator described below, it occurs at about 25 Bev. The introduction of straight sections between sectors will modify this transition point, and may increase it above the top energy limit. Otherwise, it is reasonably certain that the radiofrequency phase can be shifted at this point to avoid a loss in intensity.

Another consequence of Eq. (8) is that the momentum spread Δp associated with a given radial aperture ΔR can be very large if the n-values are large. If we use the example of $|n|=3600$, the field will vary from zero to twice its average value in a radial distance of 2 inches, with the consequence that within this aperture $\Delta p/p$ can be as large as ± 10 percent! This extremely large momentum acceptance means that at injection the errors in injection energy and in the frequency of the accelerating voltage can be of this same order of magnitude. Furthermore, it shows that the radial amplitude of the synchronous oscillations is reduced by nearly the same factor α, as compared to the ordinary synchrotron.

DESIGN CONCEPTS FOR A 30-BEV ACCELERATOR

The potentialities of this strong-focusing principle can be illustrated by describing its application to the design of a high energy accelerator. We have chosen to design for 30-Bev protons, which is 10 times the maximum energy of the Brookhaven cosmotron, and which requires an orbit radius of about 300 ft with a guide field of about 11 kilogauss. The aperture within the vacuum chamber can be as small as 1×2 inches, and still provides a safety factor of 2 over the computed maximum oscillation amplitudes. With this radial aperture the n value is determined by the radius and by the field gradient of 1.1×10^4 gauss/inch:

$$|n|=-\frac{R}{B}\frac{dB}{dr}=\frac{300\times12\times1.1\times10^4}{1.1\times10^4}=3600. \qquad (11)$$

[3] In reference 2 it is pointed out that γ can also be negative in a conventional synchrotron with straight sections.

[4] L. H. Thomas, Phys. Rev. **54**, 580, 588 (1938).

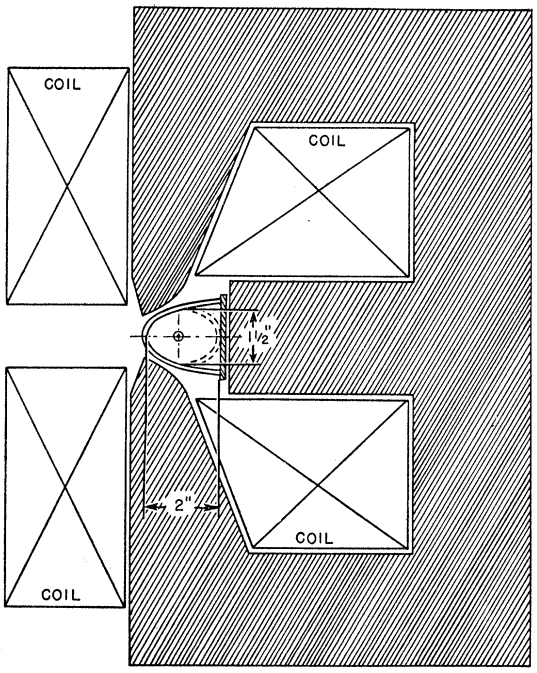

FIG. 5. Cross section of E-magnet with poles shaped to give $n=3600$ at an orbit radius of 300 ft. The vacuum chamber illustrated has an internal aperture of about 1×2 inches.

With this value of n the optimum number of magnet sectors $N=240$, and the length of each sector is 7.85 ft. We assume that short straight sections will be needed between sectors, and choose a length of 2.0 ft. The chosen injection energy of 4 Mev and the angle of divergence at injection of 10^{-3} radian, are those available from the Van de Graaff injector for the cosmotron. Detailed calculations of "betatron" oscillation amplitudes for this angle at injection, and those due to gas scattering at a residual pressure in the chamber of 1×10^{-5} mm of Hg, show that the maximum amplitudes (at injection) will be included within a square area of 0.5×0.5 inch. The radial amplitude of synchronous oscillations at injection depends on the frequency harmonic used for acceleration; a sufficiently high harmonic should be used to include the entire allowed phase oscillation range within the energy and radial limits defined by the chamber. This energy range accepted by the 2-inch radial aperture is found to be ± 10 percent, which is larger than the practical energy spread of the injector by a large factor. The conclusion from such studies is that the 1×2 inch aperture is entirely adequate for the chamber.

The basic magnet structure chosen to provide the large magnetic field gradients is a "3-pole" magnet with a single return circuit which can be called an "E-magnet," illustrated in Fig. 5. Two poles are shaped as rectangular hyperbolas, and the third "pole" is a vertical surface of iron along the vertical axis of the hyperbolas to maintain zero field at the center of the

coordinate system (the inner wall of the vacuum chamber). Between these poles the field has the property of equal and uniform gradients in the radial and vertical directions, as long as the iron surfaces remain magnetic equipotentials. The field at the center of the chamber, along the 2-inch gap chosen for the basic aperture, is considered the guide field. At injection the magnetic field at the center is about 30 gauss, and the field varies from 60 gauss to zero along the 2-inch radial extent of the aperture. As the field approaches saturation in the iron at the tips, the area of uniform-gradient, high n-value field will shrink to a smaller aperture, estimated to be no less than 1 inch. However, at such high energies, the oscillation amplitudes will be sufficiently damped so that aperture requirements are much smaller, and no loss in intensity should result. Model studies of the magnet will be required to determine the exact shape of pole faces for maximum extent of useful field at injection and the maximum practical value of guide field. For the design calculations this maximum guide field is assumed to be 11 kilogauss across the 2-inch gap, leading to a requirement of 4.5×10^4 ampere turns for excitation.

The alternation of field gradients in successive sectors can be accomplished by assembling the magnets alternately with outside and inside return legs, using the E-shape described above. Figure 6 is an illustration, not to scale, of this alternate assembly of outside-E and inside-E magnets. The center line along the axis of the chamber is on the circle of 300-ft radius, and is the axis of reversal of alternate sectors. This assembly retains many of the advantageous features of the C-magnet design. The magnet gap is available along its entire length for measurements, and the open side provides access for vacuum testing and for inspection. Injection is possible at small angles of inflection, even though the connecting straight sections are short. Ejection of a tangential emergent beam is simplified, and radiations, such as charged mesons from targets within the aperture, can be emitted through the thin chamber walls for experimental studies. On the other hand, the magnetic disadvantages of the C-magnet, which apply to the uniform-n accelerator, are largely averaged out by the use of alternating E's. The decrease in aperture due to fringing fields as the iron approaches saturation is now largely cancelled, and the primary effect is a reduction of n-values and a slight

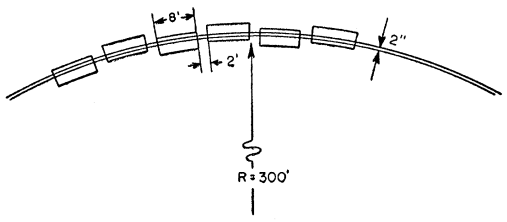

FIG. 6. Method of assembly of alternately inside-E and outside-E magnets around an orbit, with straight sections between sectors.

decrease in the focusing forces as particles approach maximum energy. Variations in the n-value due to remanent fields and eddy currents are unimportant. Thick iron laminations can be used, of 1- or 2-inch plate, determined by the economics of magnet construction.

The cross-sectional area assigned to the magnet windings is set by the power rating of the coil. Several factors enter in choosing the magnitude of the power. The primary consideration is the cost of the power, which is a significant item in operating costs. Another is the advantage to be gained by reducing the coil heating per unit length sufficiently to make water- or air-cooling of the coil windings unnecessary. Both these factors indicate a large coil cross section which means a large initial cost for the conductors and a proportionate increase in the dimensions and costs of the iron return circuit. It can also be argued that the power consumption per cycle should not exceed the circulating power required to provide the stored energy in the magnetic field. These features require detailed analysis and balancing. For the purposes of this study, we have chosen to use about half the power rating and the same duty cycle as for the present cosmotron, or 300 kilowatts averaged over a duty cycle of 1 sec up, 1 sec down, repeated at 5-sec intervals. With these assumptions the required cross section of copper windings is about 24 in.^{2} Following the design shapes illustrated in Fig. 5 we find that the E-magnet iron has external dimensions of about 12 inches wide by 20 inches high, approximately the size illustrated in the figure. Since the cross section of iron is about $\frac{1}{10}$ that of the cosmotron, the total weight of iron is about the same; the weight of copper in the windings is increased by about a factor of 5.

The acceleration voltage required to attain 30-Bev energy in 1 second is about 100 kilovolts per turn, or 100 times larger than that for the cosmotron. It is clear that many accelerating units must be used, distributed around the orbit and properly phased, primarily to reduce the radiofrequency power. It is also likely that a high harmonic of the orbital frequency would be advantageous. The radial amplitude of synchronous oscillations will be reduced by the factor $h^{-\frac{1}{2}}$, where h is the order of the harmonic. The harmonic order should be a submultiple of the number of accelerating units around the orbit, in order to simplify the problems of phasing. Several methods of applying the accelerating field to the particles are available. That used in the cosmotron involves a ferrite-loaded cavity; in this case, with sectors of 8-ft length, one might use the metal-pipe vacuum chamber as a "drift tube." The driving frequency increases with time as in the cosmotron, and must be modulated over a frequency ratio of 1 to 12. The broad-band power amplifiers used to drive the accelerating units will be one of the most difficult and costly components.

The frequency tolerance is given by

$$\frac{\Delta f}{f}=\frac{|\alpha-E_0^2/E^2|}{\alpha}\frac{\Delta L}{L}=\left|\frac{E^2-E_1^2}{E^2}\right|\frac{\Delta L}{L}. \quad (12)$$

At injection and at energies small compared with the phase-reversal energy E_1, the allowable frequency error is large, and the frequency cycle can be "pre-cut." However, as the energy approaches E_1 the allowed error becomes very small, and precision methods of frequency control will be required. Electrical pick-up pulses from the beam of particles can be used for this frequency control, as can be demonstrated with the cosmotron.

The vacuum chamber can be constructed of thin-walled, nonmagnetic tubing, such as stainless steel. The effect of eddy currents will be negligible. Such a chamber can serve many purposes. As indicated, it can serve as a "drift tube" for radiofrequency acceleration. Units can also be utilized as sensing electrodes to observe the beam pulses. Such a thin metal-walled tube can be heated and out-gassed under vacuum to reduce the residual pressure in the chamber. Small vacuum pumps can be located at the straight sections between sectors at 10-foot intervals.

The injector assumed in this study is the equivalent of the present cosmotron 4-Mev Van de Graaff generator, although it is possible that higher energies would be helpful, as from a linear accelerator. Injection could be accomplished by electrical deflection at a small angle at one of the straight sections. The time interval for acceptance, about $\frac{1}{3}$ of a turn, is about 10 microseconds. Pulse injection at 1 milliampere would result in about 5×10^{10} particles being accepted, equivalent to the intensity per pulse of the present cosmotron. The radial contraction per turn at injection would be about 1 mm at 4 Mev, which seems large enough to result in a reasonable capture efficiency. The strong focusing and damping during further acceleration will retain the beam within the aperture, even through the synchrotron phase-reversal point. It seems probable that final intensities will be equivalent to those obtained with the cosmotron.

ION FOCUSING IN LINEAR SYSTEMS

An extension of the theory of magnetic focusing by successive reversals of field gradients leads to concepts which are applicable to ion optics and to linear accelerators. The principle involves a similar sequence of alternately converging and diverging magnetic lenses, and can be visualized most readily by considering the analogy to lens optics. A single region of inhomogeneous magnetic field which produces convergence of an ion beam in one plane will produce divergence in the plane at right angles. Consider a beam of ions having a momentum $p=BR$ (where R is the radius of curvature in a field B), moving in the x direction in a field with components: $B_x=0$, $B_y=kz$, and $B_z=ky$. The equations of motion, which are equivalent to Eqs. (2) for the circular orbit, become

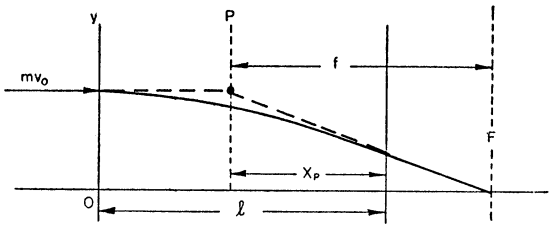

FIG. 7. Definition of focal length f and principal plane distance x_P for a convergent magnetic lens of length l.

$$\frac{d^2y}{dx^2}+\frac{1}{BR}\frac{dB_z}{dy}y=0, \quad \text{or} \quad \frac{d^2y}{dx^2}+Ky=0; \quad (13a)$$

$$\frac{d^2z}{dx^2}-\frac{1}{BR}\frac{dB_y}{dz}z=0, \quad \text{or} \quad \frac{d^2z}{dx^2}-Kz=0. \quad (13b)$$

The lens property of such a field is illustrated in Fig. 7, which shows the path of a particle entering the field parallel to the axis, in the convergent xy plane. If the length of the region of inhomogeneous field is l, the particle crosses the axis at F (the focal point), converging from a point P which defines the principal plane. The distance to the principal plane x_p and the focal length f measured from this plane are given by

$$x_P=\frac{1-\cos K^{\frac{1}{2}}l}{K^{\frac{1}{2}}\sin K^{\frac{1}{2}}l}, \quad (14)$$

$$f=\frac{1}{K^{\frac{1}{2}}\sin K^{\frac{1}{2}}l}, \quad (15)$$

where K defines the unit of length and is given by

$$K=\frac{1}{BR}\frac{dB_y}{dz}=\frac{1}{BR}\frac{dB_z}{dy}. \quad (16)$$

A sequence of two lenses of this class, separated by a distance q between principal planes, having coefficients K_1 and K_2 and lengths l_1 and l_2, will have a focal length given by the familiar lens equation

$$1/F=1/f_1+1/f_2-q/f_1f_2. \quad (17)$$

It can be noted at this point that F is positive, and so the combination of lenses is converging, if $f_2=-f_1$. This means that two equally strong converging and diverging lenses will be convergent. Applying this to the magnetic lens case by inserting the relations for principal plane distances and focal lengths for the two lenses, the combined focal length becomes

$$1/F=K_1^{\frac{1}{2}}\sin K_1^{\frac{1}{2}}l_1\cos K_2^{\frac{1}{2}}l_2+K_2^{\frac{1}{2}}\sin K_2^{\frac{1}{2}}l_2\cos K_1^{\frac{1}{2}}l_1 -dK_1^{\frac{1}{2}}K_2^{\frac{1}{2}}\sin K_1^{\frac{1}{2}}l_1\sin K_2^{\frac{1}{2}}l_2. \quad (18)$$

In this expression the distance d is the distance of sepa-

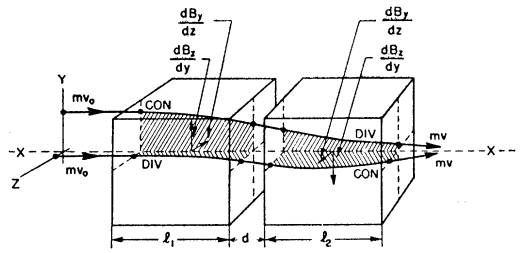

FIG. 8. Illustration of double-focusing in two magnetic lenses with field gradients in opposite directions, showing the alternately convergent and divergent forces and the net convergence of the system.

ration between the faces of the two magnetic lenses. If, for a simple example, we choose $-K_2=K_1=K$ and $l_2=l_1=l$, the equation for focal length reduces to

$$1/F=K^{\frac{1}{2}}\{\sinh K^{\frac{1}{2}}l\cosh K^{\frac{1}{2}}l-\sinh K^{\frac{1}{2}}l\cos K^{\frac{1}{2}}l+dK^{\frac{1}{2}}\sinh K^{\frac{1}{2}}l\sinh K^{\frac{1}{2}}l\}. \quad (19)$$

The condition that the lens system be convergent is that the argument $K^{\frac{1}{2}}l$ be positive and not greater than some value approaching π, depending on the magnitude of the separation distance d. Thus, the lens can be designed for any desired focal length by suitable choice of $K^{\frac{1}{2}}l$ and d. In this simple case where the K's and l's are equal, the focal lengths are equal for displacements in both the xy and xz planes, as becomes evident when $-K$ is substituted for K in Eq. (19). However, the locations of the principal planes will differ, depending on whether the initial action is converging or diverging. This leads to an astigmatic image in the simple case assumed. This astigmatism can be corrected by modifying the lens system. The double focusing of the compensating lenses is illustrated in Fig. 8, showing alternately divergent and convergent forces in the two sections.

A doubly-divergent magnetic field having uniform and equal values of dB_z/dy and dB_y/dz exists between the poles of a 4-pole magnet with pole faces shaped as rectangular hyperbolas; the field is zero along the x axis. Figure 9 shows a cross section of such a magnet. The complete lens would consist of two such magnet units of length l, with the second unit rotated by 90° relative to the first. The effective aperture of such a lens would be a circle of diameter $D=(2)^{\frac{1}{2}}a$, where a is the spacing between the centers of the hyperbolic poles. Consider a numerical example in which the aperture, a, is 2 inches and the maximum field across this 2-inch gap is 10 kilogauss. The field gradient $dB/dy=dB/dz=10^4$ gauss/inch. Let us design a magnet to focus protons of 4-Mev energy, which have a momentum BR of about 10^5 gauss-inches, so $K=0.1$. If we choose $K^{\frac{1}{2}}l=\pi/4$, and the spacing d is 2 inches, the length of each magnet unit l is 2.5 inches, the total length is 7.0 inches, and the focal length computed from Eq. (19) is 4.4 inches. Choice of a smaller value of $K^{\frac{1}{2}}l$ will lead to shorter magnets and longer focal lengths. A simpler relation for computing focal lengths can be

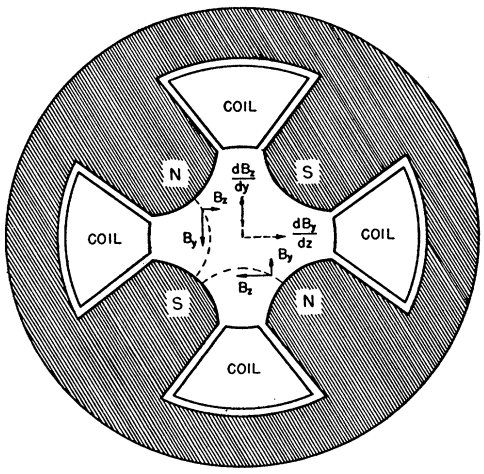

FIG. 9. Cross section of a 4-pole magnet with hyperbolic pole faces to produce uniform and equal field gradients dB_z/dy and dB_y/dz.

obtained from Eq. (19) by expanding in terms of the arguments and using only the first significant terms:

$$1/F=K^2l^2\{\tfrac{2}{3}l+d\}. \quad (20)$$

A continuous sequence of such convergent systems is itself convergent if the separation distance D between successive image and object focal points is less than $\pm 2F$. This relationship is equivalent to that given in Eq. (4) for the circular orbit. Thus, magnetic lenses of the type described can be used in succession to maintain a focused beam over long distances, as in the linear accelerator.